Electronic Supporting Information

Azaacene Containing Iridium(III) Phosphors: Elaboration of π-Conjugation Effect and Application in Highly Efficient Solution-Processed Near-infrared OLEDs

Min Li,[a] Li Wang,[b] Caifa You,[b*] Denghui Liu,[b] Kai Zhang,[b] and Weiguo Zhu[b*]

[a] Jiangxi Province Key Laboratory of Polymer Micro/Nano Manufacturing and Devices, School of Chemistry and Materials Science, East China University of Technology, Nanchang, 330013, Jiangxi, P. R. China.

[b] School of Materials Science and Engineering, Jiangsu Engineering Laboratory of Light-Electricity-Heat Energy-Converting Materials and Applications, Jiangsu Key Laboratories of Environment-Friendly Polymers, National Experimental Demonstration Center for Materials Science and Engineering, Changzhou University, Changzhou 213164, P. R. China.

Email addresses: youcaifa0710@163.com; zhuwg18@126.com

Table of Contents

1. Experimental Section

1.1 Materials and methods

All reagents and chemicals were purchased from commercial sources and used directly without any further purification unless stated otherwise. Intermediates **1** and **2** were synthesized according to previously reported literature.[1, 2] Column chromatography was carried out with Merck silica gel (200 – 300 mesh). Thin-layer chromatography (TLC) with Merck pre-coated was adopted to monitor reactions until the reactants were consumed completely. All reactions were performed under a nitrogen atmosphere to avoid the oxidation of the reactants by oxygen.

^{1}H-NMR and ^{13}C-NMR spectra were recorded at room temperature on Bruker Avance III NMR spectrometer and the chemical shifts (δ) are reported in parts per million (ppm) using tetramethyl silane (TMS) signals as internal standards. Matrix-assisted laser desorption ionization time of flight mass spectrometry (MALDI-TOF-MS) was performed with Bruker Daltonics AutoflexTM III using α-cyano- 4-hydroxycinnamic acid (CCA) as matrix. Elemental analysis was measured with Vario EL III elementary analyzer. Cyclic voltammetry (CV) was performed using CHI630E at a scan rate of 100 mV s^{-1}. All experiments were carried out in a three-electrode compartment cell with a Pt-wire counter electrode, a Pt-disk working electrode and Ag/AgCl reference electrode. The supporting electrolyte used was 0.1 M tetrabutylammonium hexafluorophosphate (Bu_4NPF_6) solution in dry acetonitrile under a nitrogen atmosphere using ferrocene (Fc) as the calibrant. The (HOMO)and (LUMO) levels are calculated by assuming the energy level of ferrocene/ferrocenium to be -4.8 eV. The thermal gravimetric analysis (TGA) was performed on a TA Instruments (TGA 50) under nitrogen gas flow with a heating rate of 20 ^{o}C min^{-1}. Ultraviolet-Visible (UV-Vis) absorption spectra were carried out on Shimadzu UV-2600 spectrometer. Steady-state photoluminescence (PL) measurements were recorded on Edinburgh Instruments (FLS1000), while phosphorescence decay lifetimes were carried out using time-correlated single-photon counting (TCSPC) spectrometer (DeltaFlex-01-DD/HORIBA) after removing the oxygen in the solution by vacuum

technique (three freeze-pump-thaw cycles), and delta diode laser 510 nm were used as excitation source. Phosphorescence at 77 K was measured on Edinburgh Instruments (FLS1000) in 2-MeTHF frozen matrix. The photoluminescence quantum yields (PLQYs) of iridium complex are measured in degassed CH_2Cl_2 solutions using a calibrated integrating sphere.

All calculations are carried out with Gaussian 09 software package using a spin-restricted formalism. The ground states of the complexes were calculated using density functional theory (DFT) and time-dependent DFT (TD-DFT) at the TPSSH/ Def2SVP level.

1.2 Preparation of NIR-emitting devices

The structure of iridium(III) complexes doped PLEDs is ITO/ PEDOT: PSS (40 nm)/ poly-TPD (30 nm)/ (PVK: OXD-7, 7: 3]: complex (x wt%, 80 nm)/ TmPyPB (50 nm) / CsF (0.8 nm)/Al (120 nm). In these devices, indium-tin-oxide (ITO) is anode, poly(3,4-ethylenedioxythiophene): polystyrene sulfonate (PEDOT: PSS) is employed as hole-injection layer (HIL), poly[bis(4-phenyl) (4-butylphenyl)amine] (poly-TPD) is acted as hole-transporting layer (HTL). Poly (*N*-vinyl carbazole): 2,2'-(1,3-phenylene)-bis[5-(4-tert-butyl-phenyl)-1,3,4-oxadiazole] (PVK: OXD-7) is served as co-host. x wt% represents the ratios of iridium complexes doped into PVK: OXD-7. 1,3,5-Tri[(3-pyridyl)-phen-3-yl]benzene (TmPyPB) is served as an electron-transporting layer (ETL) and hole-blocking layer (HBL). Caesium fluoride (CsF) is used as an electron-injection layer (EIL) and aluminum (Al) is acted as a cathode. PEDOT: PSS films are spin coated on precleaned ITO glass substrates and annealed at 120 °C for 20 min (thickness: 40 nm). It is then covered by poly-TPD (30 nm). Subsequently, a blend of PVK: OXD-7 and dopants in chlorobenzene solution is spin-coated on top of the poly-TPD with a thickness of 80 nm. TmPyPB films are then spin-coated on the active layer with a thickness of 50 nm. Finally, CsF/ Al electrodes are thermally evaporated through a shadow mask. The active area is 4 mm^2 for each PLED. The PLEDs are encapsulated in a glove box prior to the device characterization. The CBP hosted NIR-OLEDs with a

device structure of ITO/ PEDOT: PSS (40 nm)/ TAPC (50 nm)/ CBP: Ir complex (y wt%, 60 nm) / TmPyPB (50 nm)/ CsF (1.2 nm)/ Al (120 nm) are fabricated from solution-processed method. In this NIR-OLED, cyclohexylidene bis[*N*,*N*-bis(p-tolyl)aniline] (TAPC) used as the HTL. The light-emitting layer consisted of iridium complex and 4,4'-bis(*N*-carbazolyl)-1,1'-biphenyl (CBP) host.

1.3 Measurements of NIR-emitting devices

The EL spectra and current density (*J*)-voltage (*V*)-Radiance (*R*) curves are obtained using a PHOTO RESEARCH Spectra Scan PR 735 photometer and a KEITHLEY 2400 Source Meter constant current source at room temperature. The EQE values are done from the radiance, current density, and EL spectrum on the premise of a Lambertian distribution.

1.4 Synthesis

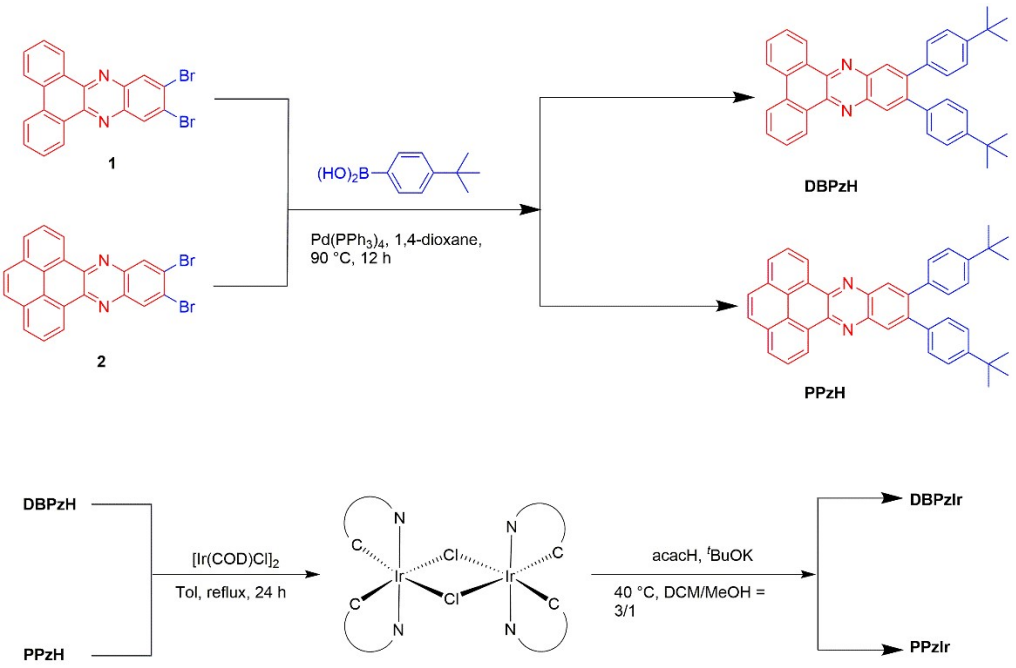

Scheme S1. Synthetic procedures for C^N ligands and iridium(III) complexes.

General synthesis procedure for Suzuki-Miyaura coupling reaction

Under nitrogen atmosphere, a mixture of 1 eq. intermediate **1** or **2**, 2.1 eq. of (4-(tert-butyl)phenyl)boronic acid, and 8% eq. of $Pd(PPh_3)_4$ were dissolved into 1,4-

dioxane, then an aqueous solution of K_2CO_3 (2 M, 6 eq.) was added, the resulting reaction mixture were heated at 90 °C, after the completely consumption of the staring materials (monitored by TLC), the reaction mixture was cooling to room temperature and wash with brine, extracted with dichloromethane (2 × 20 mL). The combined organic phase was dried over anhydrous $MgSO_4$ and solvents were removed under reduced pressure. The crude mixture was then purified by chromatography on silica gel with petroleum ether/dichloromethane mixture as eluent to furnish ligand **DBPzH** and **PPzH**.

DBPzH: PE/DCM (3/1, v/v) as eluent, yellow-green solid, 91% yield. ^{1}H NMR (400 MHz, $CDCl_3$, δ): 9.41 (dd, J = 7.8, 1.2 Hz, 2H), 8.58 (d, J = 7.8 Hz, 2H), 8.37 (s, 2H), 7.82 – 7.73 (m, 4H), 7.31 (d, J = 8.4 Hz, 4H), 7.24 (d, J = 8.4 Hz, 4H), 1.34 (s, 18H). ^{13}C NMR (125 MHz, $CDCl_3$, δ): 150.19, 143.53, 142.57, 141.54, 137.74, 131.98, 130.45, 130.22, 130.19, 129.79, 127.92, 126.31, 124.93, 122.91, 34.66, 31.49. MS (MALDI-TOF) $[M+H]^+$: calcd for $C_{40}H_{37}N_2$: 545.288; found: 545.488. Elemental analysis calculated for $C_{40}H_{36}N_2$: C, 88.20; H, 6.66; N, 5.14; found: C, 88.23; H, 6.76; N, 5.27.

PPzH: PE/DCM (3/1, v/v) as eluent, yellow solid, 85% yield. ^{1}H NMR (400 MHz, $CDCl_3$, δ): 9.55 (t, J = 7.7 Hz, 2H), 8.39 (d, J = 3.2 Hz, 2H), 8.29 – 8.22 (m, 2H), 8.07 (dt, J = 12.4, 6.1 Hz, 2H), 8.02 (d, J = 5.5 Hz, 2H), 7.32 (d, J = 8.3 Hz, 4H), 7.26 (d, J = 5.5 Hz, 4H), 1.35 (s, 18H). ^{13}C NMR (125 MHz, $CDCl_3$, δ): 150.23, 143.60, 143.32, 141.71, 137.76, 131.36, 130.25, 129.82, 129.61, 129.02, 127.15, 126.79, 125.99, 124.95, 123.91, 34.68, 31.51. MS (MALDI-TOF) $[M+H]^+$: calcd for $C_{42}H_{37}N_2$: 569.288; found: 569.313. Elemental analysis calculated for $C_{42}H_{36}N_2$: C, 88.69; H, 6.38; N, 4.93; found: C, 88.53; H, 6.41; N, 4.90.

General synthesis procedure for iridium(III) μ-chloro-dimer complexes

Under N_2 atmosphere, 1 eq. of chloro(1,5-cyclooctadiene)iridium(I) dimer $(Ir(COD)Cl)_2$ and 4 eq. of ligand **DBPzH** or **PPzH** were refluxed at 115 °C for 24 h in 25 mL toluene. The reaction mixture slowly turned to dark black. Toluene was removed under reduced pressure after cooling to room temperature. Without further

purification, the dimer was used directly for the next reaction.

General procedure for the synthesis of the studied iridium(III) complexes

1 eq. of the corresponding μ-chloro-dimer, 2 eq. of acetylacetone (acacH) and 2.5 eq. of ^{t}BuOK were added into 20 mL of mixture of dichloromethane and methanol (*V*/*V* = 3/1). Then the reaction mixture was refluxed under N_2 atmosphere overnight. After cooling down to room temperature, the mixture was extracted with dichloromethane and washed by distilled water. The solution was dried over anhydrous $MgSO_4$ and the solvent was evaporated to dryness. The residual was purified by flash column chromatography using petroleum ether/dichloromethane as the eluent. Finally, dark black solid was obtained. All these complexes were further purified by recrystallization from methanol and dichloromethane mixture, followed by vacuum drying process before characterization.

DBPzIr: PE/DCM (2/1, v/v) as eluent, dark black solid, 30% yield. ^{1}H NMR (400 MHz, $CDCl_3$, δ): 9.45 – 9.41 (m, 2H), 8.80 (s, 2H), 8.53 – 8.45 (m, 4H), 7.96 (d, *J* = 7.8 Hz, 2H), 7.83 – 7.74 (m, 4H), 7.31 (t, *J* = 9.0 Hz, 8H), 7.09 (d, *J* = 8.4 Hz, 4H), 7.04 – 6.95 (m, 6H), 6.65 (d, *J* = 7.6 Hz, 2H), 4.80 (s, 1H), 1.34 (s, 18H), 1.16 (s, 18H), 0.95 (s, 6H). ^{13}C NMR (125 MHz, $CDCl_3$, δ): 186.72, 156.94, 150.50, 150.29, 150.07, 144.92, 144.13, 142.66, 142.36, 142.31, 141.55, 137.49, 137.36, 133.97, 133.51, 133.12, 130.80, 129.81, 129.77, 127.74, 126.67, 126.19, 125.02, 124.82, 123.34, 114.99, 34.69, 34.50, 31.51, 31.33, 27.60. MS (MALDI-TOF) [M-acac]$^{+}$: calcd for $C_{80}H_{70}IrN_4$: 1279.523; found: 1279.324. Elemental analysis calculated for $C_{85}H_{77}IrN_4O_2$: C, 74.05; H, 5.63; N, 4.06; found: C, 74.21; H, 5.67; N, 4.09.

PPzIr: PE/DCM (2/1, v/v) as eluent, dark black solid, 23% yield. ^{1}H NMR (400 MHz, $CDCl_3$, δ): 9.57 (d, *J* = 7.7 Hz, 2H), 8.80 (s, 2H), 8.51 (s, 2H), 8.26 (d, *J* = 7.7 Hz, 2H), 8.04 (t, *J* = 7.7 Hz, 2H), 7.87 – 7.77 (m, 4H), 7.48 (d, *J* = 8.2 Hz, 2H), 7.31 (q, *J* = 8.2 Hz, 8H), 7.09 (dd, *J* = 18.4, 8.2 Hz, 6H), 6.97 (d, *J* = 8.2 Hz, 4H), 4.83 (s, 1H), 1.35 (s, 18H), 1.13 (s, 18H), 0.96 (s, 6H). MS (MALDI-TOF) [M-acac]$^{+}$: calcd for $C_{84}H_{70}IrN_4$: 1327.523; found: 1327.305. Elemental analysis calculated for $C_{89}H_{77}IrN_4O_2$: C, 74.92; H, 5.44; N, 3.93; found: C, 75.01; H, 5.39; N, 3.94.

2. Supplementary Figures and Tables

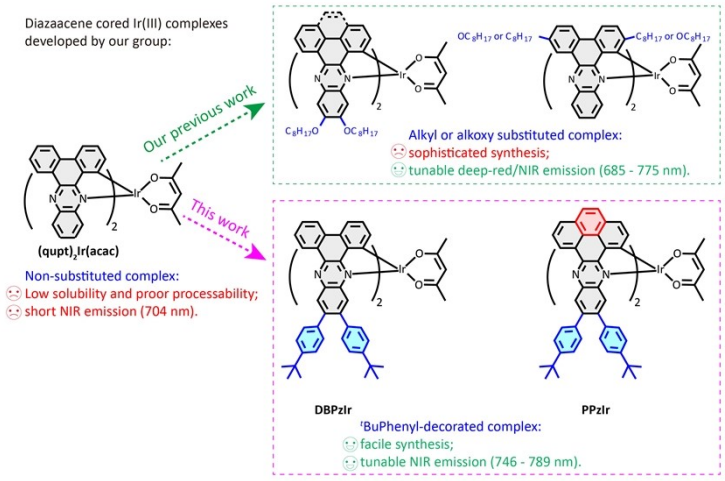

Scheme S2. Diazaacene-cored Ir(III) complexes studied in this study and their analogues in our earlier reported work.

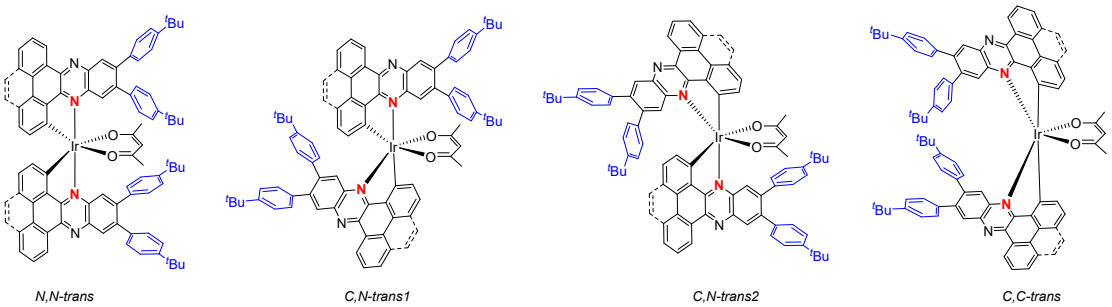

Figure S1. Possible isomer structures of $(C^N)_2Ir(acac)$-typed complexes in this study.

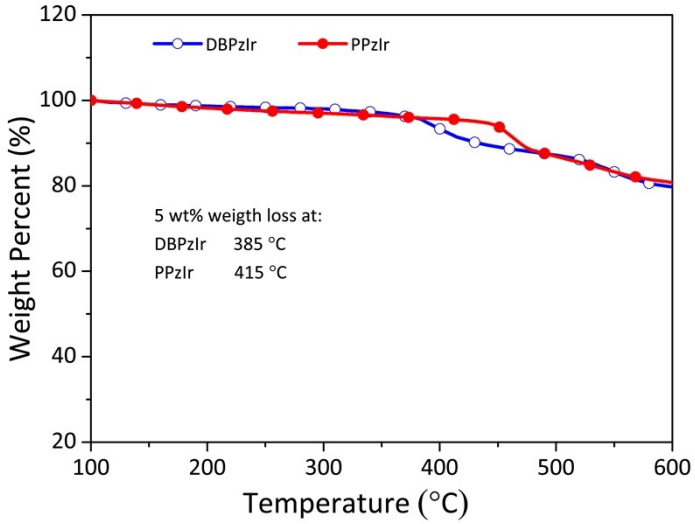

Figure S2. TGA curves under N_2 flow.

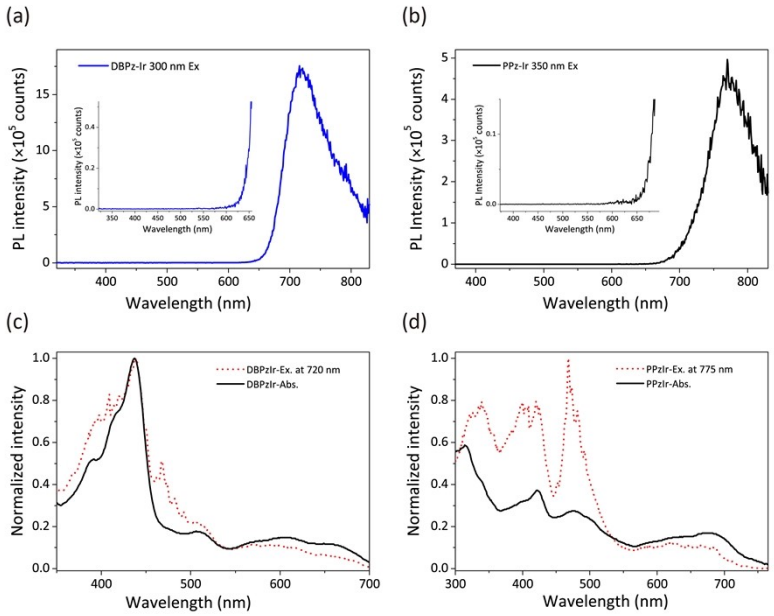

Figure S3. Emission and excitation spectra of complex **DBPzIr** (a), (c); and complex **PPzIr** (b), (d) in 10^{-5} M toluene solutions at RT. Inset: the enlarged PL spectra below 650 nm. Full PL spectra can't be obtained due to the limitation of PMT-900 detector.

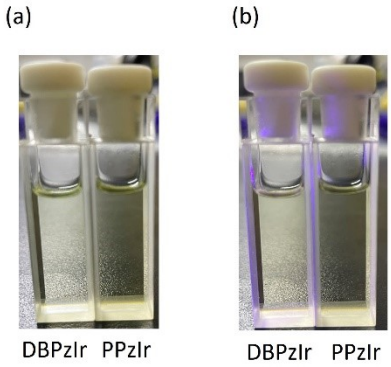

Figure S4. Photos of the studied complexes in 10^{-5} toluene under: (a) natural daylight; (b) 365 nm light. The blue light at the quartz cuvette is the reflection of 365 nm light.

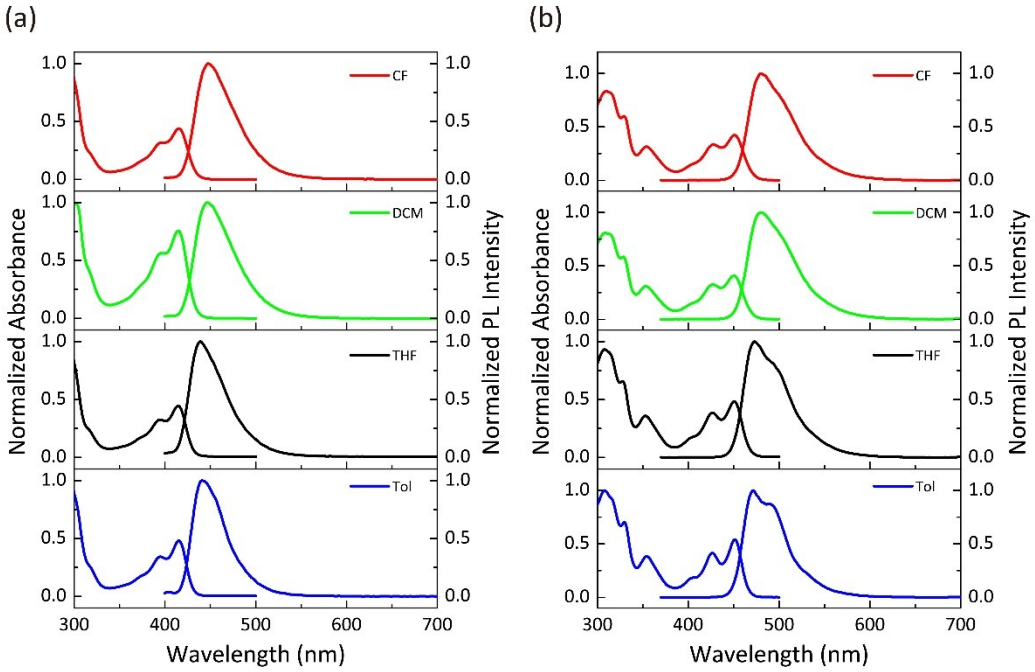

Figure S5. Absorption and emission spectra of ligand **DBPzH**, Ex = 300 nm (a) and **PPzH**, Ex = 350 nm (b) in various solvents with a concentration of 10^{-5} M at RT.

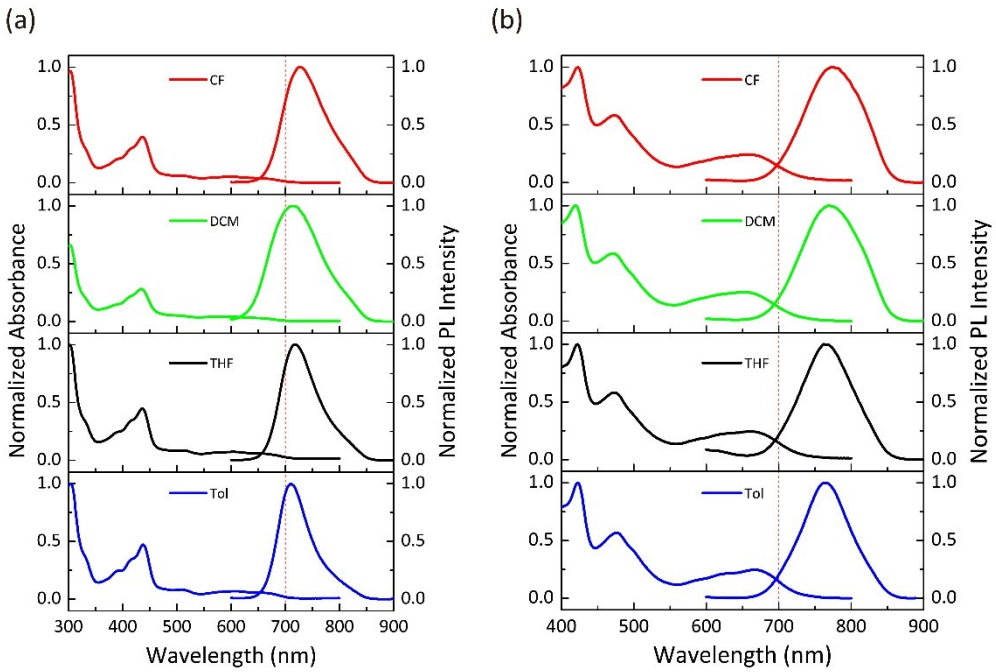

Figure S6. Absorption and emission spectra of complex **DBPzIr**, Ex = 500 nm (a) and **PPzIr**, Ex = 600 nm (b) in various solvents with a concentration of 10^{-5} M at RT.

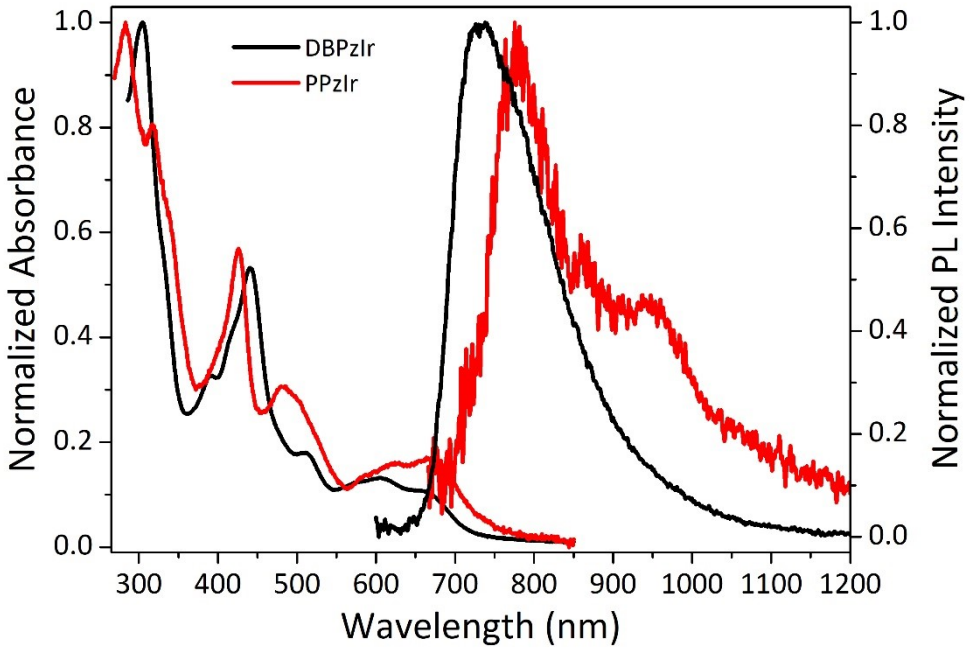

Figure S7. Normalized absorption and emission of Ir(III) complexes in neat films.

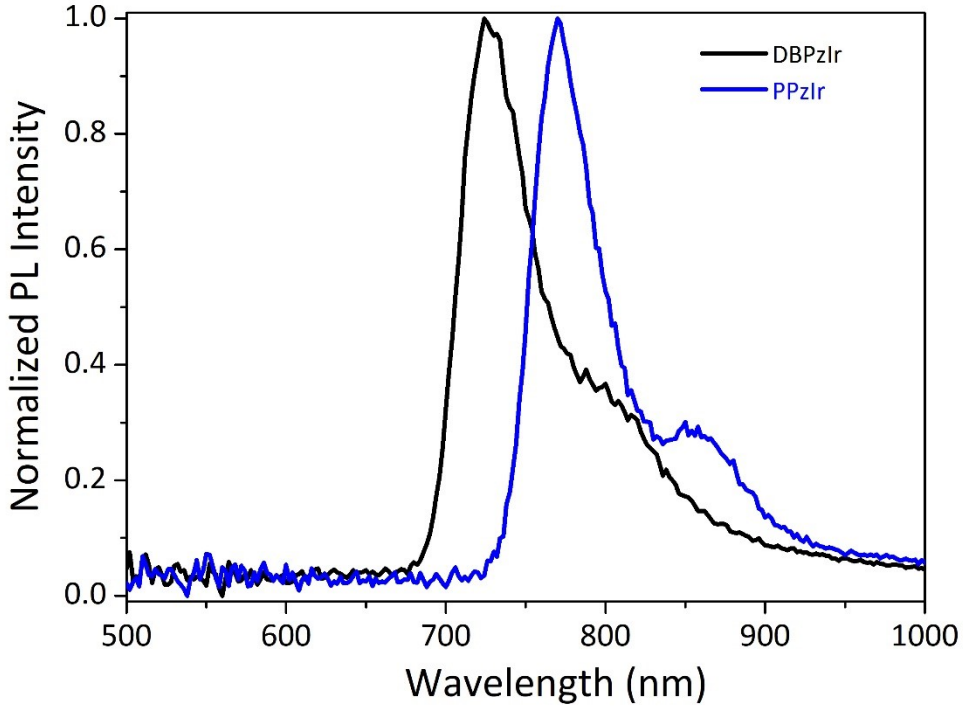

Figure S8. Normalized emission spectra of Ir(III) complexes in 10^{-5} M of 2-MeTHF matrix at 77 K.

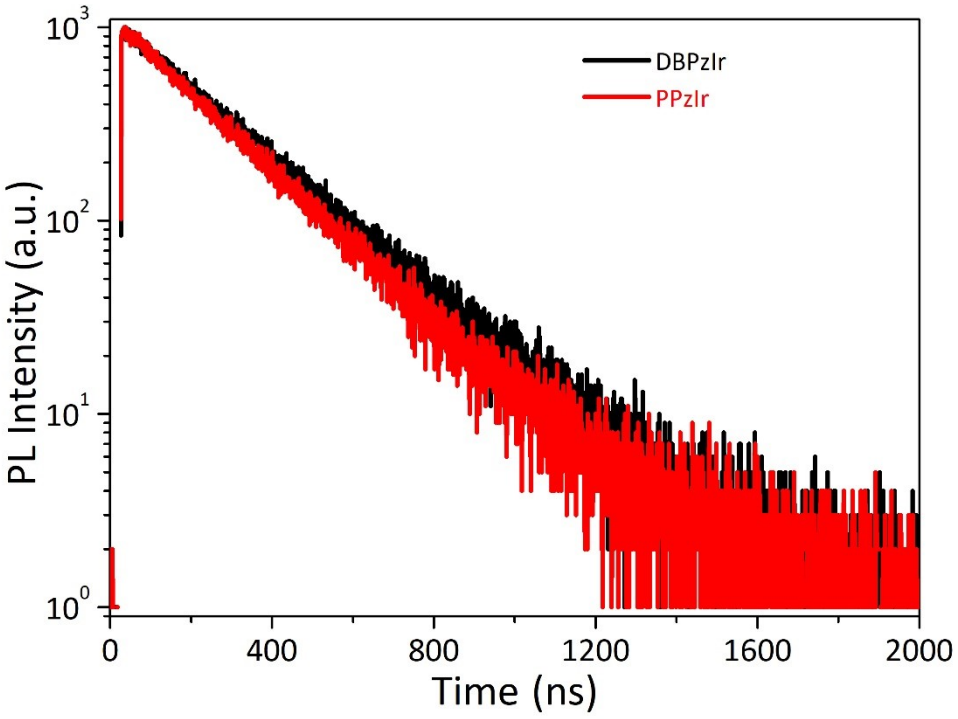

Figure S9. Transition decay curves of iridium(III) complexes in degassed CH_2Cl_2 solution.

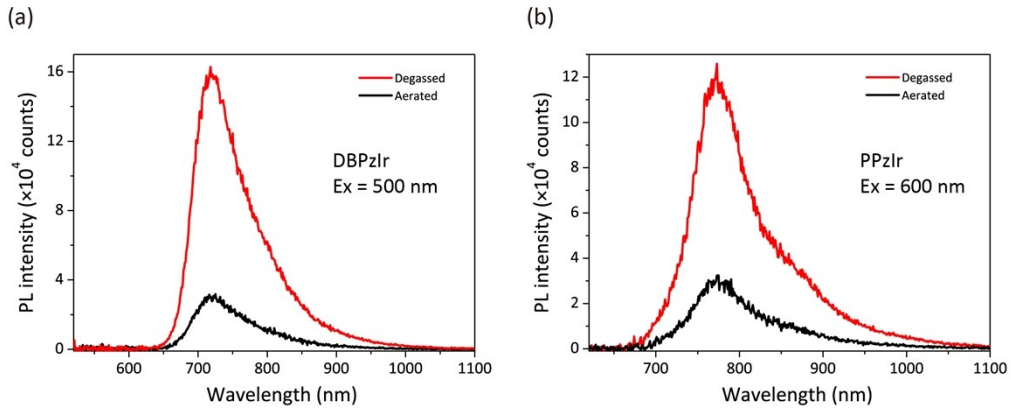

Figure S10. PL spectra of studied complexes in aerated and degassed toluene solutions.

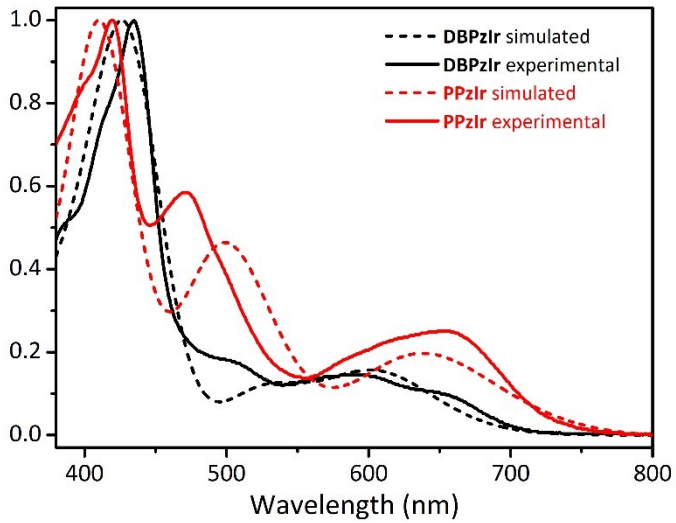

Figure S11. Experimental UV−Vis absorption spectra and simulated spectra for **DBPzIr** and **PPzIr**.

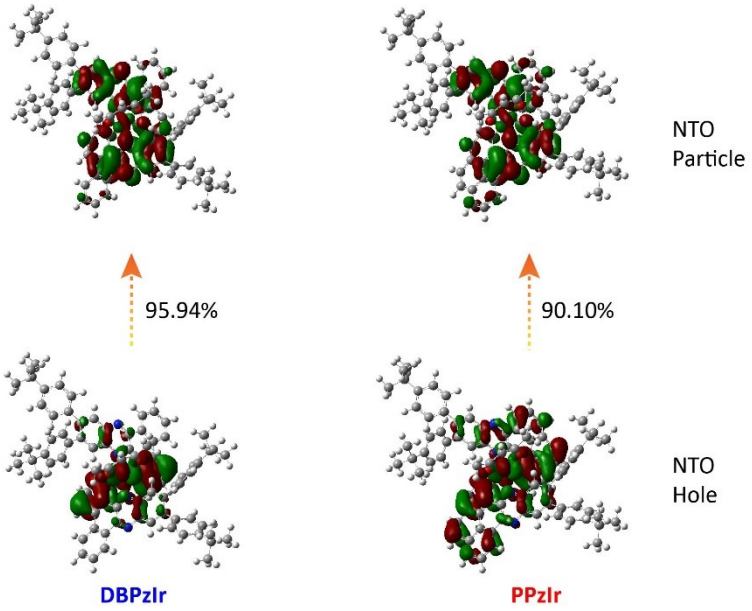

Figure S12. Natural transition orbital patterns for $S_0 \rightarrow T_1$ transitions for these studied complexes based on their optimized T_1 geometries.

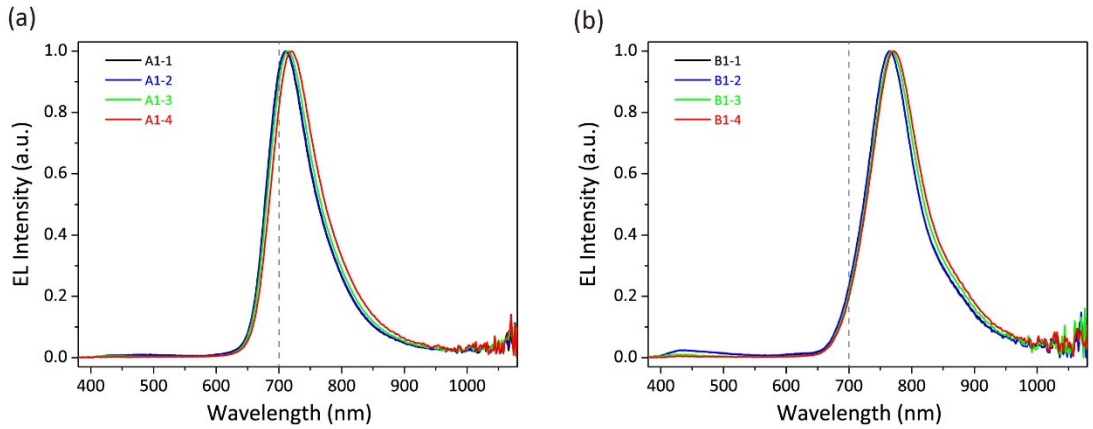

Figure S13. Normalized EL spectra of device A1 (a) and B1 (b).

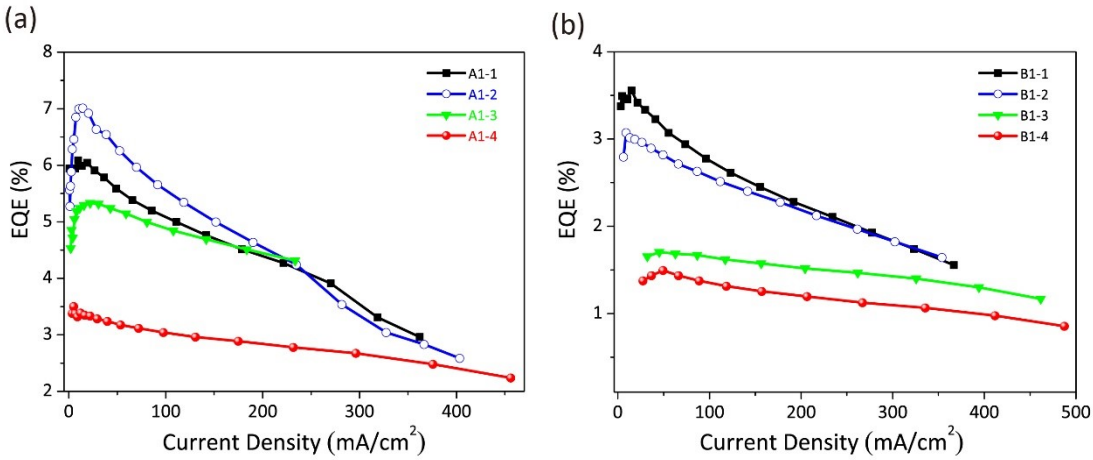

Figure S14. EQE-*J* curves of device A1 (a) and B1 (b).

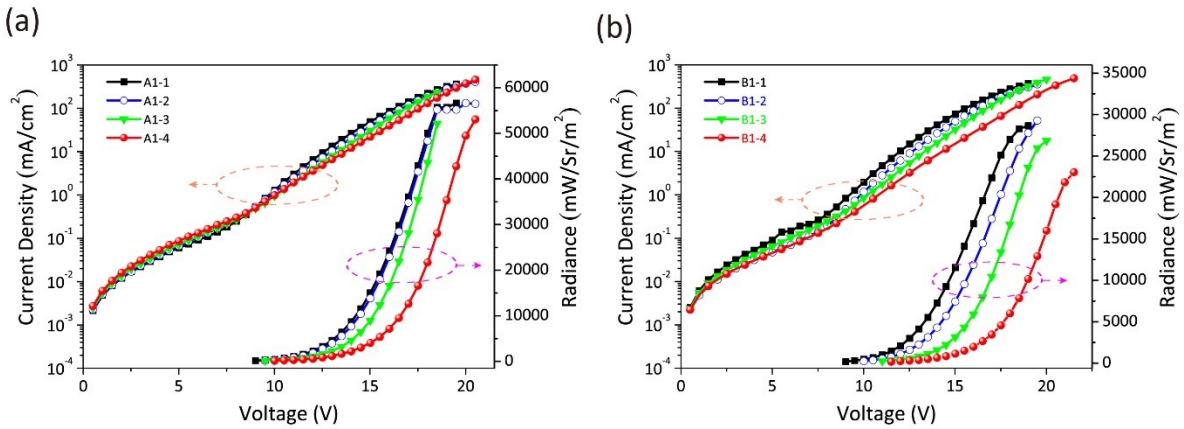

Figure S15. *J*–*V*–*R* profiles of device A1 (a) and B1 (b).

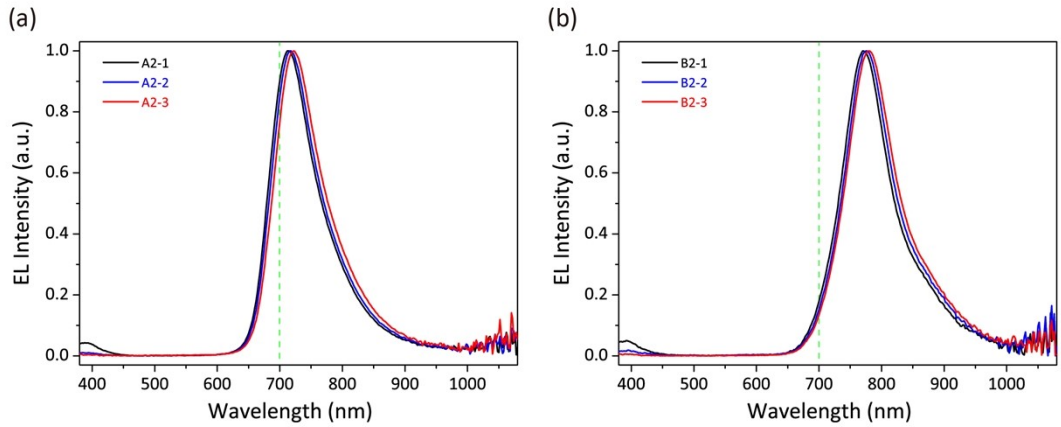

Figure S16. Normalized EL spectra of device A2 (a) and B2 (b).

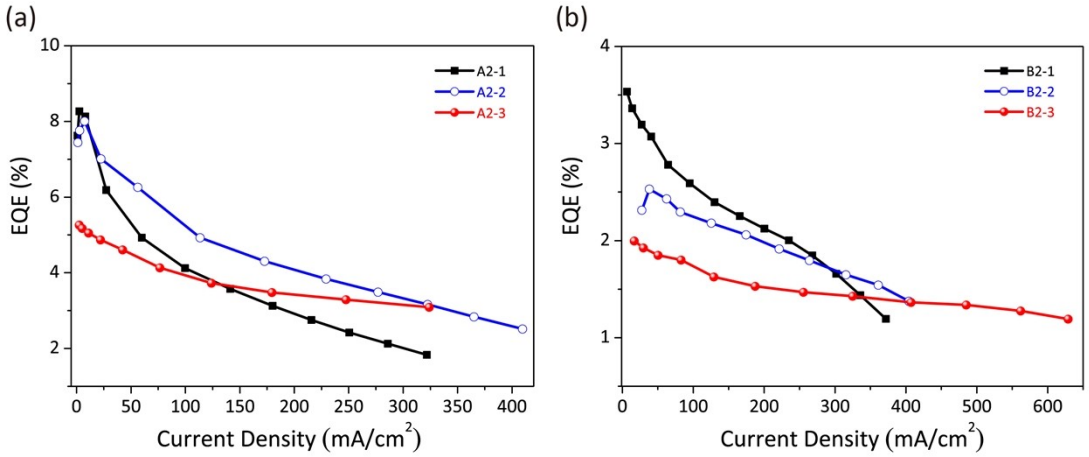

Figure S17. EQE-*J* curves of device A2 (a) and B2 (b).

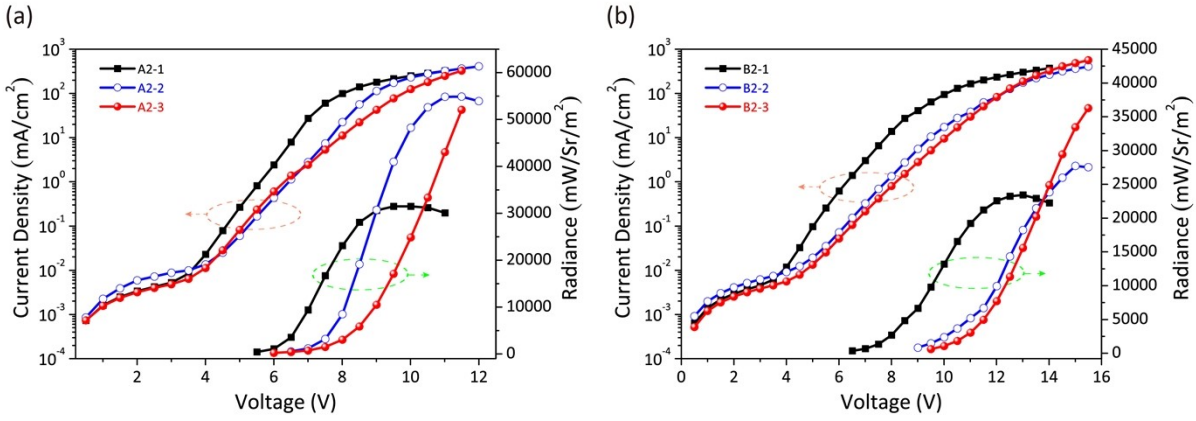

Figure S18. *J*–*V*–*R* profiles of device A2 (a) and B2 (b).

Table S1. Excited states of complex **DBPzIr** and **PPzIr** calculated by TD-DFT

Complex	State (E_{cal} (eV), λ_{cal} (nm)	Dominant excitations (%)	Oscillator strength (f)	Character
DBPzIr	S_1 (2.00, 618)	H → L (97)	0.0107	MLCT/ILCT/LLCT
	S_2 (2.04, 605)	H → L+1 (97)	0.0789	MLCT/ILCT/LLCT
	T_1 (1.77, 697)	H → L (94) H-2→ L+1 (2.6)	0	MLCT/ILCT/LLCT
	T_2 (1.85, 669)	H → L+1 (92) H-2→ L (4.0)	0	MLCT/ILCT/LLCT
PPzIr	S_1 (1.91, 648)	H → L (98)	0.0303	MLCT/ILCT/LLCT
	S_2 (1.94, 636)	H → L+1 (97)	0.0964	MLCT/ILCT/LLCT
	T_1 (1.62, 765)	H → L (89) H-1→ L+1 (8.8)	0	MLCT/ILCT/LLCT
	T_2 (1.66, 743)	H-1→ L (13) H → L+1 (8.5)	0	MLCT/ILCT/LLCT

Table S2. TD-DFT results for studied complexes based on their optimized S_0 geometries.

Complex	MOs [a]	Contribution percentages of metal d_π orbitals, ligands π orbitals to MOs/%			Main configuration of $S_0 \rightarrow S_1$ excitation /E_{cal}/λ_{cal}/f/character [b]	Main configuration of $S_0 \rightarrow T_1$ excitation /E_{cal}/λ_{cal}/character [b]
DBPzIr		Ir	C^N ligands	acac	H → L (97.36%)	H → L (94.31%)
					2.0055 eV	1.7782 eV
	L	2.78	96.67	0.55	618.21 nm	697.24 nm
					f = 0.0107	f = 0
	H	36.14	59.96	3.90	π(C-N)/d_π(Ir) → π*(C-N)	π(C-N)/d_π(Ir) → π*(C-N)
PPzIr	L	2.81	96.67	0.52	H → L (97.74%)	H → L (89.01%)
					1.9127 eV	1.6204 eV
	H	24.25	73.48	2.27	648.20 nm	765.17 nm
					f = 0.0303	f = 0
					π(C-N)/d_π(Ir) → π*(C-N)	π(C-N)/d_π(Ir) → π*(C-N)

[a] H and L denote molecular orbitals (MOs) HOMO of and LUMO, respectively; [b] E_{cal}, λ_{cal}, and f represent calculated excitation energies, calculated absorption wavelengths, and oscillator strength, respectively. And f for $S_0 \rightarrow T_1$ is zero under TD-DFT calculation without the consideration of SOC.

Table S3. NTO results for studied complexes based on their optimized T_1 geometries.

complex	NTOs [a]	Contribution percentages of metal d_π orbitals, and ligands π orbitals to NTOs/%		
		Ir	C^N ligands	acac
DBPzIr	P	3.48	95.66	0.68
	H	37.61	58.80	3.59
PPzIr	P	3.47	95.89	0.64
	H	25.85	71.94	2.21

[a] H and P represent NTO hole and particle orbital, respectively.

Table S4. Summarized electroluminescent performance of studied Ir(III) complexes with different doping concentrations.

Dopant	Ratio (wt%)	Device type	V_{on} (V)	λ_{EL}^{max} (nm)	EQE [a)] (%)	R_{max} (mW Sr^{-1} m^{-2})	NIR photos (%) [b)]
DBPzIr	0.8	A1-1	8.5	710	6.08/5.09	56615	76
	1.0	A1-2	9.0	712	7.01/5.58	56647	77
	2.0	A1-3	10.0	716	5.33/4.88	52175	79
	4.0	A1-4	10.5	720	3.50/3.05	53070	83
	1.0	A2-1	5.5	714	8.27/4.10	31488	78
	2.0	A2-2	6.5	716	8.00/5.24	54866	81
	4.0	A2-3	6.5	722	5.26/3.91	52044	85
PPzIr	0.8	B1-1	9.5	764	3.56/2.74	28654	93
	1.0	B1-2	10.0	766	3.07/2.57	29274	93
	2.0	B1-3	12.0	768	1.71/1.64	26836	96
	4.0	B1-4	13.0	770	1.49/1.34	23038	97
	1.0	B2-1	7.0	772	3.53/2.56	22258	95
	2.0	B2-2	9.0	776	2.53/2.25	27703	97
	4.0	B2-3	10.0	780	2.00/1.73	36921	98

[a)] Maximum EQE value then at 100 mA cm^{-2} current density; [b)] percentage of spectral area ≥ 700 nm.

Table S5. Device performance of diazaacene-cored Ir(III) phosphors doped devices.

Dopant	Ratio (wt%)	V_{on} (V)	λ_{EL}^{max} (nm)	FWHM [a] [nm]	EQE [b] (%)	R_{max} (mW Sr^{-1} m^{-2})	NIR emission [c]	Reference
DBPzIr	1.0	9.0	712	85	7.01/5.58	56647	77	This work
	2.0	6.5	716	91	8.00/5.24	54866	81	
PPzIr	0.8	9.5	764	91	3.56/2.74	28654	93	
	1.0	7.0	772	93	3.53/2.56	22258	95	
(DBPz11,12-DO)$_2$Ir(acac)	1.0	8.4	674	84	7.04/4.43	33671	38	*J. Mater. Chem. C* **2019**, *7*, 10961.
(PPz-11,12-DO)$_2$Ir(acac)	1.0	10.8	724	89	4.14/3.05	20981	79	
Ir-R	1.0	5.5	730	81	6.91/3.39	26100	86	*J. Mater. Chem. C* **2020**, *8*, 7079.
Ir-OR	0.8	12.5	760	104	1.45/1.16	11518	87	
Ir4	2.0	7.8	718	85	12.34/3.85	24647	81	*Adv. Opt. Mater.* **2020**, *8*, 2000154.
TPAIr	1.0	11.5	768	97	3.34/2.71	29151	96	*Chem. Eng. J.* **2023**, *452*, 138956.
HTIr	0.8	9.6	786	105	1.86/1.56	16803	98	
DPTAIr	1.0	7.0	800	94	2.98/2.00	17083	95	

[a] Full width at half maximum of EL spectrum; [b] Maximum EQE value then at 100 mA/cm^2 current density, and the corresponding efficiency roll-off values listed in brackets; [c] percentage of area ≥ 700 nm in the EL spectra.

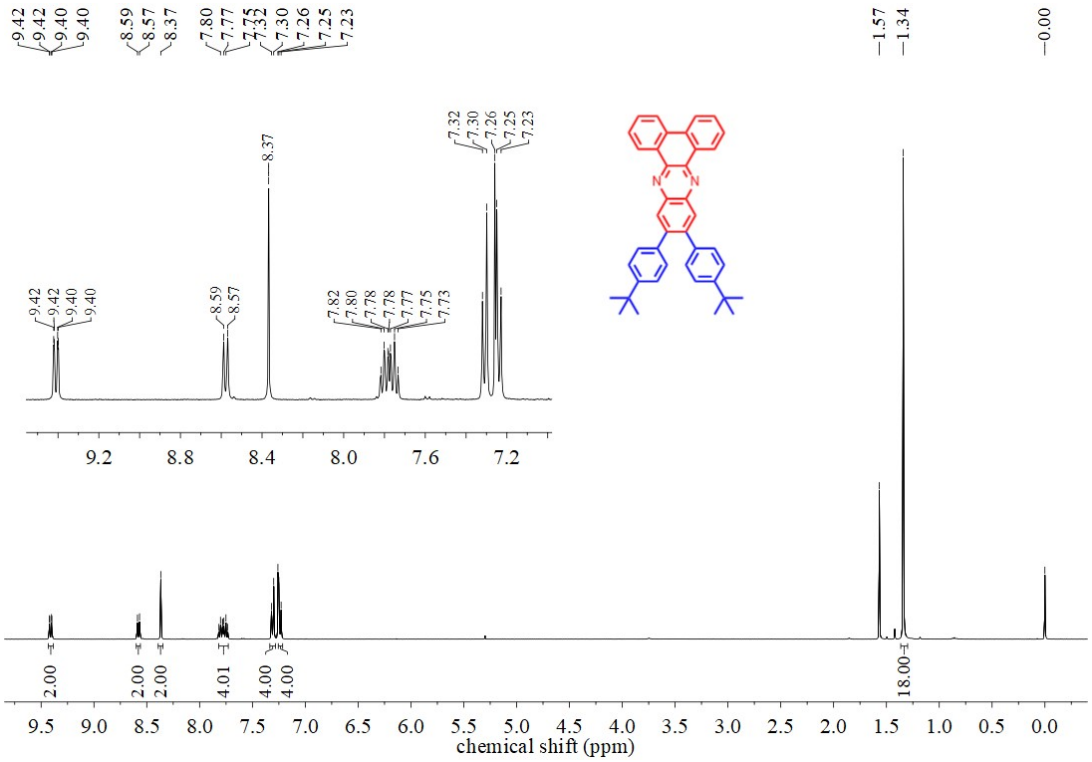

Figure S19. ^{1}H-NMR spectrum of **DBPzH** (400 MHz, $CDCl_3$, RT).

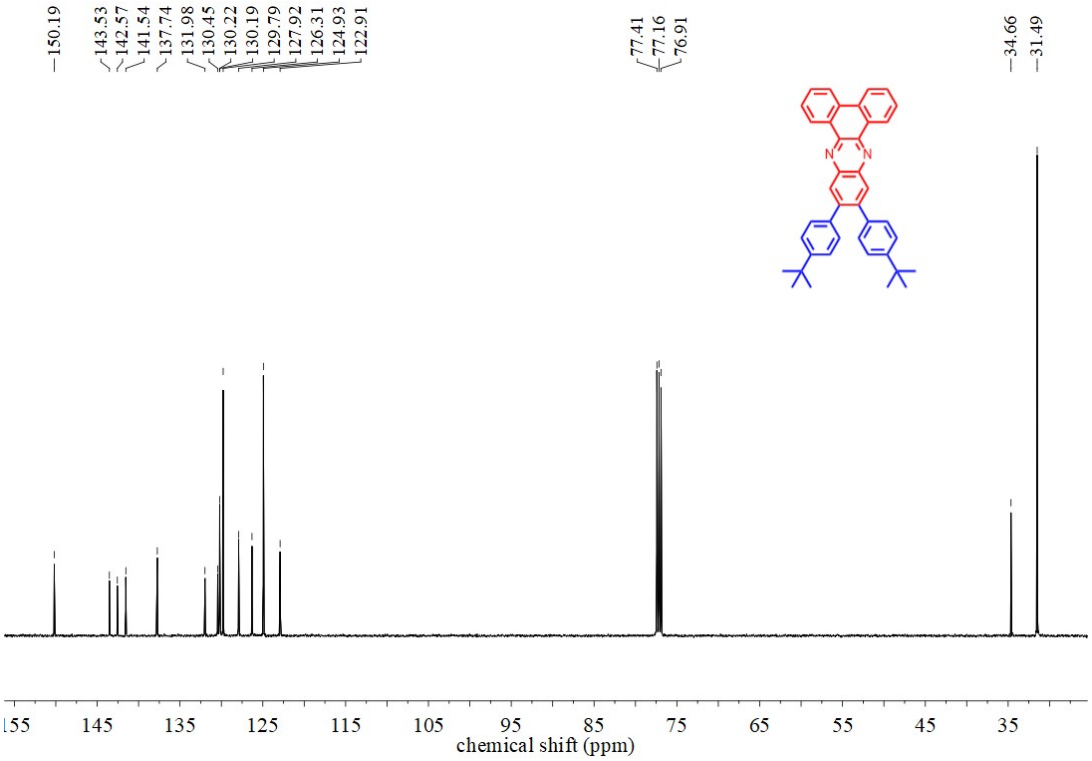

Figure S20. ^{13}C-NMR spectrum of **DBPzH** (125 MHz, $CDCl_3$, RT).

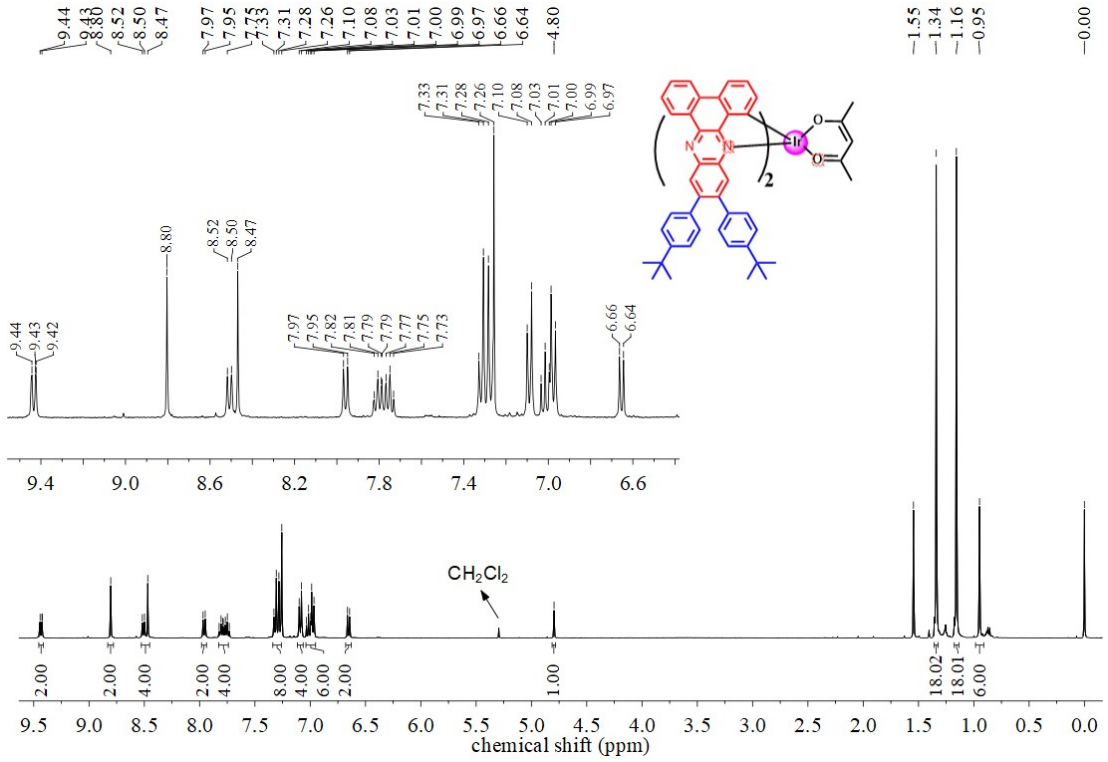

Figure S21. ^{1}H-NMR spectrum of **DBPzIr** (400 MHz, $CDCl_3$, RT).

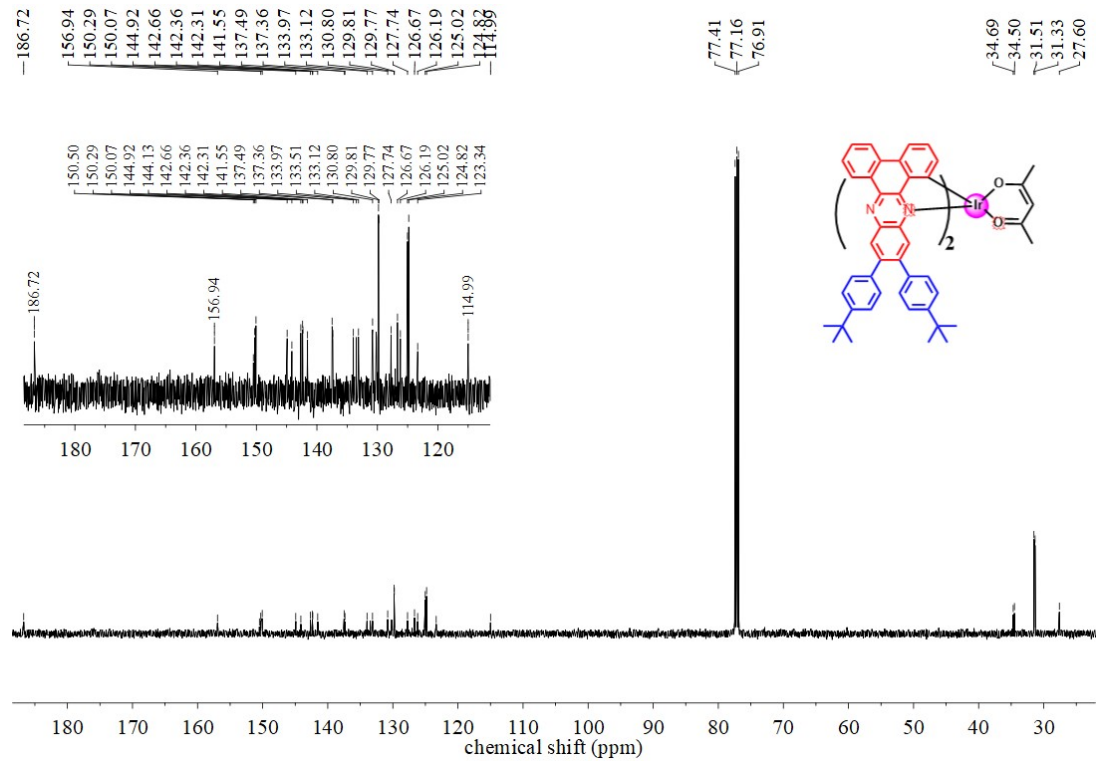

Figure S22. ^{13}C-NMR spectrum of **DBPzIr** (125 MHz, $CDCl_3$, RT).

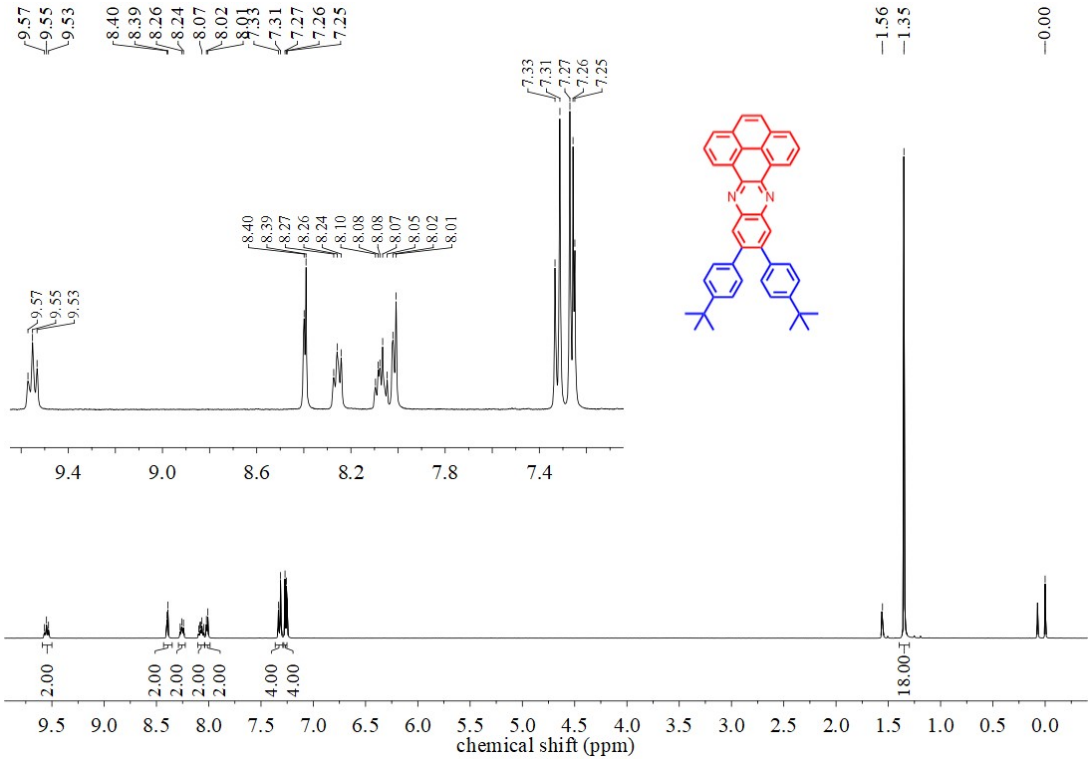

Figure S23. ^{1}H-NMR spectrum of **PPzH** (400 MHz, $CDCl_3$, RT).

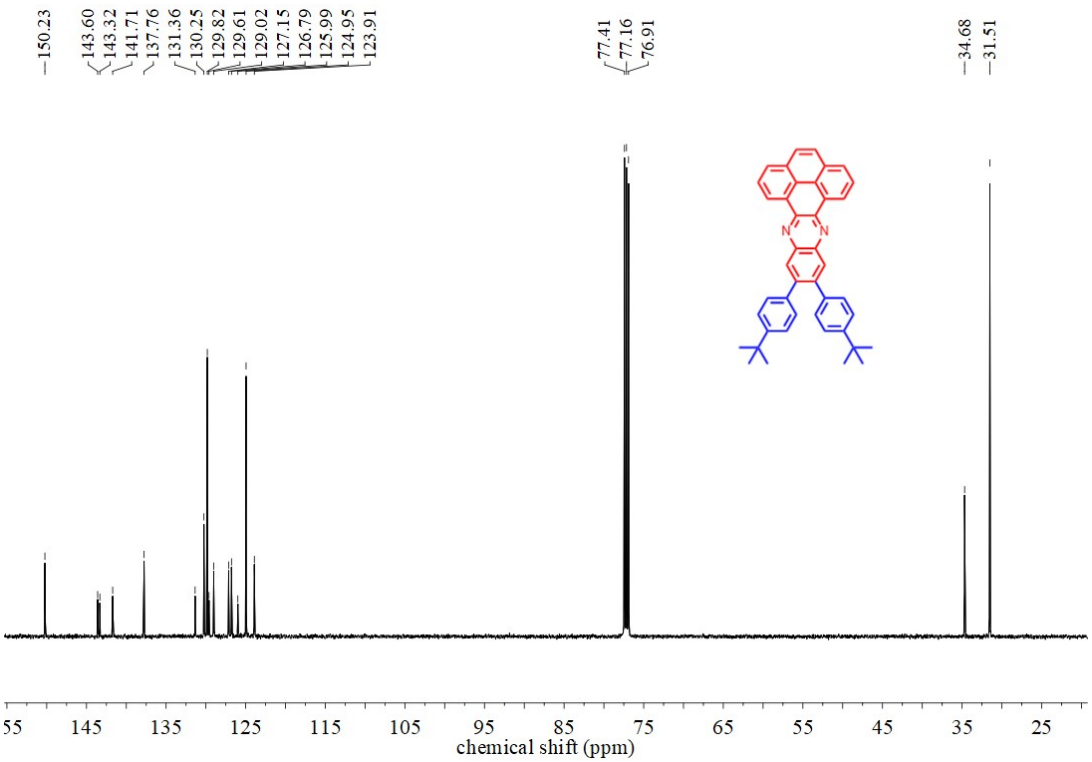

Figure S24. ^{13}C-NMR spectrum of **PPzH** (125 MHz, $CDCl_3$, RT).

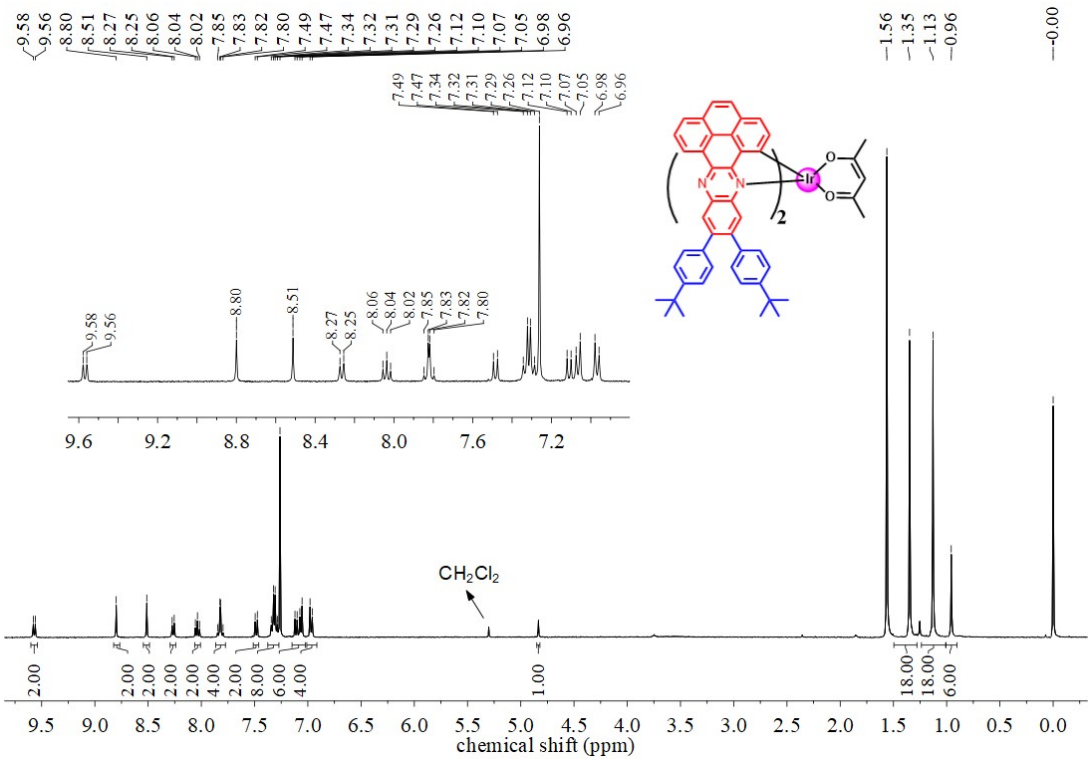

Figure S25. ^{1}H-NMR spectrum of **PPzIr** (400 MHz, $CDCl_3$, RT).

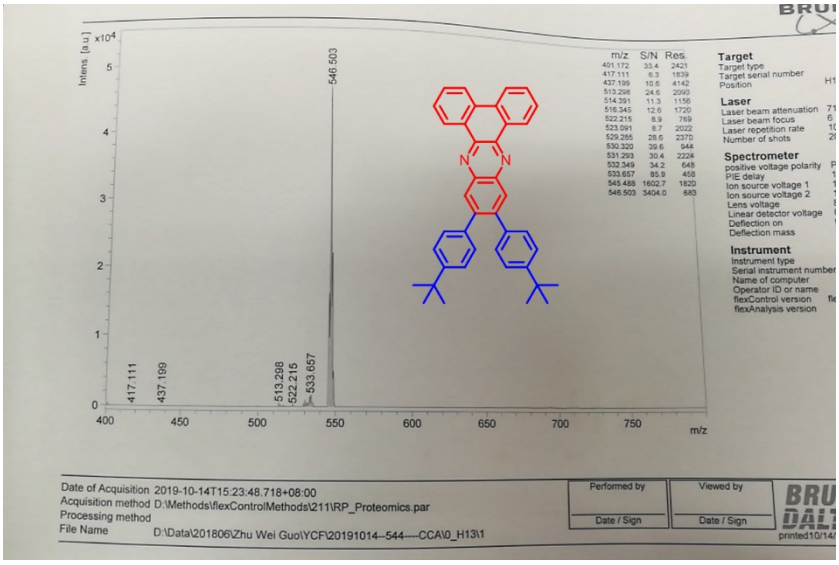

Figure S26. MALDI-TOF MS spectrum of **DBPzH**.

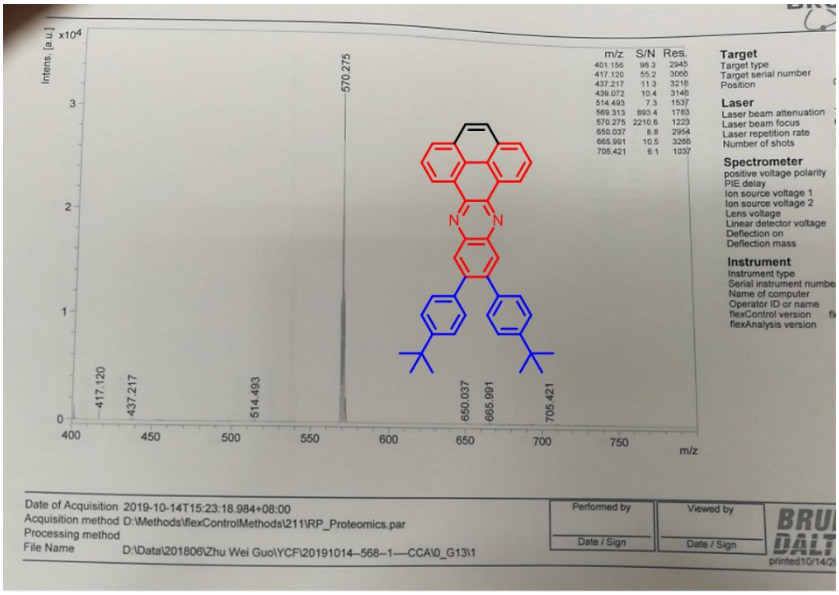

Figure S27. MALDI-TOF MS spectrum of **PPzH**.

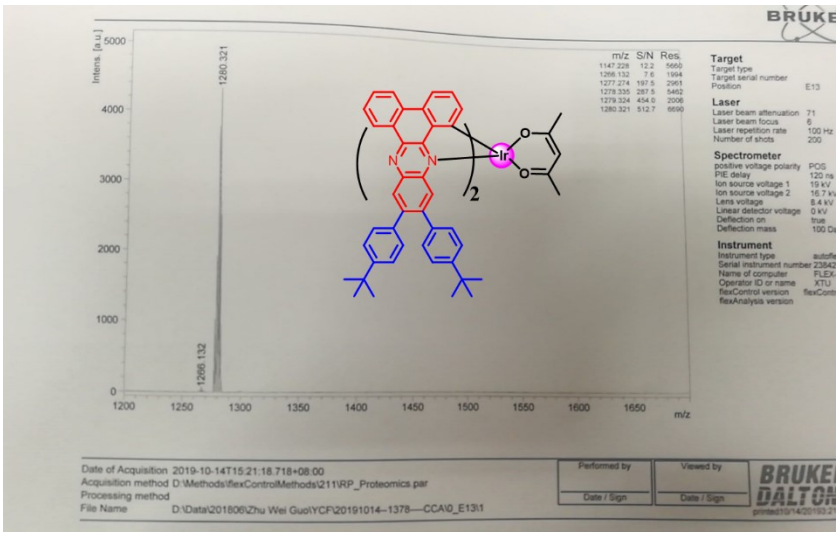

Figure S28. MALDI-TOF MS spectrum of **DBPzIr**

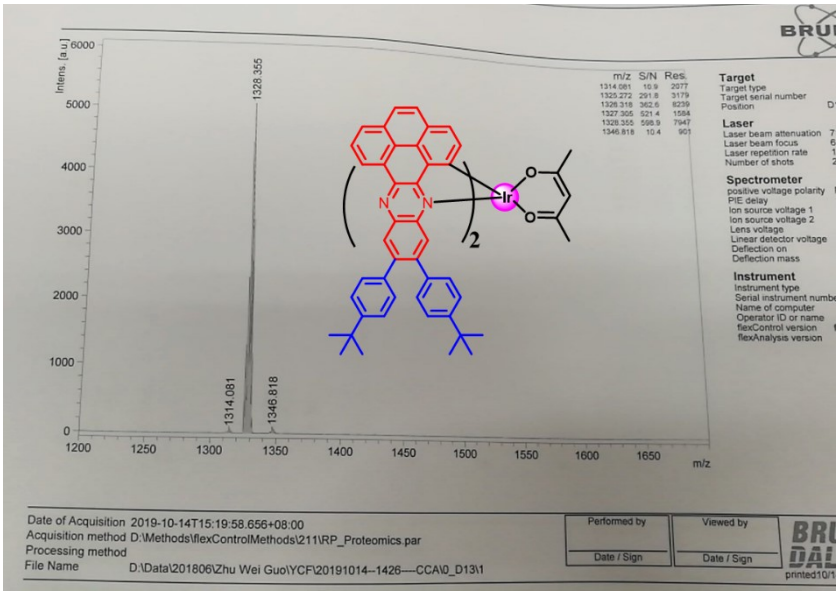

Figure S29. MALDI-TOF MS spectrum of **PPzIr**

3. References

1 B. Gao, Y. Liu, Y. Geng, Y. Cheng, L. Wang, X. Jing and F. Wang, *Tetrahedron Lett.*, 2009, **50**, 1649-1652.

2 P. K. Sahoo, C. Giri, T. S. Haldar, R. Puttreddy, K. Rissanen and P. Mal, *Eur. J. Org. Chem.*, 2016, **2016**, 1283-1291.